

Mobility Analysis of Electrons in CF_4 by FTI Method

Akihide TAKEDA and Nobuaki IKUTA¹

Shikoku University, Ohjin, Tokushima 771-11

¹Tokushima University, Minamijousanjima, Tokushima 770

(Received January 14, 1993)

Due to large cross sections for vibrational excitation which sharply rise in the bottom region of the Ramsauer minimum, electrons in CF_4 in low reduced electric fields E/N show particular transport properties. The transport property and velocity distribution of electrons in CF_4 are analysed using the FTI method of the authors over a wide range of E/N from 0.1 to 50 Td. The mobility, drift velocity and the negative differential conductivity are discussed with the flight behavior of electrons regarding the variation of elastic and inelastic collision frequencies with energy.

[anisotropy, mobility, negative differential conductivity, Ramsauer minimum, CF_4 , FTI method]

§1. Introduction

CF_4 is an important gas in the industrial use in processing plasma for semiconductor device manufacturing. At the same time, it is an interesting gas having sharp rises of vibrational excitation cross sections within the Ramsauer valley similarly to such as in CH_4 , SiH_4 and GeH_4 . Electron drift velocities in these gases have a particular shape with a hump in a region of low reduced electric field E/N , and have a region of negative differential conductivity (NDC) on the right hand side of the hump. The hump and NDC in the drift velocity— E/N curves are observed not only in gases such as CH_4 , SiH_4 and CF_4 , but also in diluted molecular gases in argon having a Ramsauer minimum. While, the cause and the features of the hump and NDC in the drift velocity curves were discussed by Petrovic *et al.*¹⁾ and Robson²⁾ using model cross sections without a minimum in the momentum transfer cross section.

Electron drift velocity in pure CF_4 was measured by Naidu and Prasad³⁾ (1972), Christophorou⁴⁾ (1979), Nakamura⁵⁾ (1990), and in diluted CF_4 with Ar by Nakamura⁶⁾ (1992), while the measurement of longitudinal diffusion coefficient has been first performed by Nakamura.^{5,6)} A set of electron collision cross sections of CF_4 have been reported at first by Hayashi⁷⁾ (1987), and also by

Nakamura⁸⁾ (1988). According to the experimental data in diluted CF_4 gas in Ar, Nakamura⁹⁾ analized a new vibrational cross sections giving a second peak in the vibrational cross section q_{v13} , and Hayashi has also reported a set of revised cross sections mainly through the beam data.¹⁰⁾ These cross sections, however, do not seem to be able to give good agreement to both the drift velocity and the longitudinal diffusion coefficient. The present authors have analysed the transport properties of electrons in CF_4 by adopting the flight time integral (FTI) method of the authors. Our aim is not to evaluate the quality of these cross sections but only to know the feature of CF_4 cross sections giving particular transport properties for electrons.

We analysed the electron transport behavior in CF_4 over a wide range of reduced E/N from 0.1 to 50 Td. Here, 1 Td is $1 \times 10^{-17} \text{ Vcm}^2$. In the E/N range below 1 Td, a high mobility is observed and its peak value exceeds $10^7 \text{ m}^2 (\text{Vs})^{-1}$ at about 0.2 Td of E/N with the mean energy below 0.1 eV. It was found that the high mobility is not caused by a high anisotropy in the velocity distribution but is caused mainly by the low collision frequency of electrons below 0.1 eV and the negative gradient of electron collision frequency. In the medium E/N range between 1 and 20 Td, highly anisotropic velocity distributions are observed with the increase of drift velocity with a

hump at about 20 Td. NDC is observed in the higher E/N region above 20 Td where the total collision frequency increases. In this paper, not only the numerical results but also the variation of electron transport properties in these regions are discussed from the flight behavior. It is emphasized to be important to consider the flight behavior of electrons with reference to the cross sections to understand the particular variation of transport properties in this peculiar gas.

§2. Flight Time Integral (FTI) Method

FTI method¹¹⁾ is a powerful procedure to obtain the velocity distribution and transport coefficients of electrons¹²⁾ and ions¹³⁾ in equilibrium state due to its accuracy and stability. In this method, the flight behavior of electrons (ions) is fully considered with the instantaneous collision frequency. This method consists of three steps, the preparation of velocity dispersion functions through a flight and a collision, relaxative determination of normalized starting rate distribution $\Psi_{sn}(v_0)$, and finally the calculation of velocity distribution and transport properties. The flight behaviors of electrons under an electric field are described

accurately with the “velocity dispersion functions through a flight” $H(v', v_0)$, and the change of velocity through a scattering is described by the “velocity dispersion function through a collision” $S(v'_0, v')$. Electrons in equilibrium state have a steady velocity distribution $F(v)$ accompanied with a starting rate distribution $\Psi_s(v_0)$. It is convenient to normalize $\Psi_s(v_0)$ to be $\Psi_{sn}(v_0)$ as below. The adoption of $\Psi_{sn}(v_0)$ as the principal unknown function is the original feature of the FTI method, and it allows to know the accurate flight behavior of electrons from the start to next collision using the velocity dispersion functions calculated following the instantaneous collision frequency under given conditions. $\Psi_{sn}(v_0)$ is obtained through repetitive operations of the loop dispersion function $L(v'_0, v_0)$ as the result of relaxation.

$$\begin{aligned}\Psi_{sn}(v'_0) &= \lim_{k=1}^m [S(v'_0, v') \otimes H(v', v_0)]^k \otimes \Psi_{sn}(v_0), \\ &= \lim_{k=1}^m [L(v'_0, v_0)]^k \otimes \Psi_{sn}(v_0), \quad (v'_0 \rightarrow v_0)\end{aligned}\quad (1)$$

where

$H(v', v_0)$: velocity dispersion function through a flight started from v_0 ,
$S(v'_0, v')$: velocity dispersion function through a collision at v' ,
$L(v'_0, v_0)$: loop velocity dispersion function through a flight and a collision from v_0 to v'_0 ,
$\Psi_{sn}(v_0) = \Psi_s(v_0) / \langle v \rangle$: normalized starting rate distribution,
$\Psi_s(v_0)$: Actual starting rate distribution,
$\langle v \rangle$: mean collision frequency,
\otimes	: overlap integral in full velocity range.

Isotropic scattering of electrons in the laboratory frame is usually assumed in the FTI analysis, where the functions above are simplified to be $H(v', v_0)$, $S(v'_0, v)$, $L(v'_0, v_0)$ and $\Psi_{sn}(v_0)$. Therefore, $H(v', v_0)$ is written as a function to give the velocity dispersion probability to dv' at v' for an electron isotropically started from v_0 at angle θ_0 referred to the direction of the electric force.

$$H(v', v_0) \equiv \int_0^\pi \int_0^\infty v_T(\tau) \exp \left(- \int_0^\tau v_T(\tau') d\tau' \right) \delta(\tau - t) d\tau (1/2) \sin \theta_0 d\theta_0, \quad (2)$$

where $v_T(\tau)$ is the total collision frequency of the electron at τ , and $\delta(\tau - t)$ is the delta function giving the value of the integrand to a small velocity division dv' at v' at time t . On the other hand, $S(v'_0, v')$ is obtained by considering the velocity change through a scattering.¹²⁾ Consequently, the loop velocity dispersion functions $L(v'_0, v_0)$ give the results of cascading velocity dis-

persions through a flight and a collision, and the repeated application of them to an arbitrary initial distribution gives a normalized starting rate distribution in equilibrium state $\Psi_{Sn}(v_0)$ quite naturally. The number of repetitive operation m of $L(v'_0, v_0)$ is usually stopped when the sum of absolute differences between $\Psi_{Sn}(v_0)_{m-1}$ and $\Psi_{Sn}(v_0)_m$ in respective v_0 divisions reduces to less than 10^{-8} .

When $\Psi_{Sn}(v_0)$ is determined, the velocity distribution of an electron swarm $F(v)$, $F(v_x)$ etc. are calculated by using an overlap-integration of the velocity dispersion functions within a flight $Hf_l(v, v_0)$ to $\Psi_{Sn}(v_0)$

$$\begin{aligned} F(v) &= \sum_{l=0}^{\infty} F_l(v), \\ &= \sum_{l=0}^{\infty} Hf_l(v, v_0) \otimes \Psi_{Sn}(v_0), \end{aligned} \quad (3)$$

$$Hf_l(v, v_0) \equiv \int_0^\pi \int_0^\infty (2l+1) P_l(\cos \theta(\tau)) \exp \left(- \int_0^\tau v_T(\tau') d\tau' \right) \delta(\tau-t) d\tau (1/2) \sin \theta_0 d\theta_0, \quad (4)$$

where,

$$\cos \theta(t) = v_x(t)/v(t), \quad (5)$$

$$v_x(t) = v_0 \cos \theta_0 + at, \quad (6)$$

$$v(t) = [v_0^2 + 2v_0 \cos \theta_0 at + a^2 t^2]^{1/2}. \quad (7)$$

Here "a" is the acceleration rate eE/m for an electron, and "e" and "m" are the electronic charge and mass, respectively.

$F(v_x)$ is obtained using the velocity dispersion functions $Hf(v_x, v_0)$ as

$$F(v_x) = Hf(v_x, v_0) \otimes \Psi_{Sn}(v_0), \quad (8)$$

where $Hf(v_x, v_0)$ is given in the same formula for $Hf_0(v, v_0)$ delivering the values of integrand to each $v_x(t) dv_x$.

The mean values of quantity z just before a collision and the mean values of z through a flight for an electron started with v_0 are obtained by transport functions $Gz(v_0)$ and $Gfz(v_0)$ as,

$$Gz(v_0) \equiv \int_0^\pi \int_0^\infty z v_T(\tau) \exp \left(- \int_0^\tau v_T(\tau') d\tau' \right) d\tau (1/2) \sin \theta_0 d\theta_0, \quad (9)$$

$$Gfz(v_0) \equiv \int_0^\pi \int_0^\infty z \exp \left(- \int_0^\tau v_T(\tau') d\tau' \right) d\tau (1/2) \sin \theta_0 d\theta_0. \quad (10)$$

Mean values of z for an electron just before a collision and through a flight are obtained as

$$\langle Gz \rangle = \int_0^\infty Gz(v_0) \Psi_{Sn}(v_0) dv_0, \quad (11)$$

$$\langle Gfz \rangle = \int_0^\infty Gfz(v_0) \Psi_{Sn}(v_0) dv_0 / \langle Gf1 \rangle. \quad (12)$$

From the values of $\langle Gz \rangle$ and $\langle Gfz \rangle$, all the transport data are easily calculated. For example, the drift velocity W and the mean energy $\langle \epsilon \rangle$ in flight are given using the simple average of flight time $\langle Gf1 \rangle$.¹²⁾

$$W = \langle Gx \rangle / \langle Gt \rangle = \langle Gfv_x \rangle / \langle Gf1 \rangle, \quad (13)$$

$$\langle \epsilon \rangle = \langle Gf\varepsilon \rangle / \langle Gf1 \rangle. \quad (14)$$

Accordingly, the energy and momentum balances are also verified in detail in the FTI method, of course.

The variable v in FTI analyses is easily replaced by the energy ε , and both the procedure using v and ε give the same results. The theory of the FTI method has been described in 1993¹³⁾ and the effectiveness was reported in 1990.¹²⁾

§3. Results and Discussion

FTI analyses have been carried out over the E/N range between 0.1 and 50 Td, where the effect of electron attachment and ionization on the transport properties is considered negligible. We have adopted the collision cross sections of CF_4 reported by Hayashi,¹⁰⁾ where rotational cross sections are not given as well as in CH_4 and SiH_4 . Cross sections used here are listed in Table I and shown in Fig. 1 as functions of energy ε . Here, the variable ε is used instead of v . The gas density of 10^{17} cm^{-3} has been assumed. The mobility (μ) curve referred to E/N has a maximum value exceeding $10^7 \text{ cm}^2(\text{Vs})^{-1}$ at about 0.2 Td as shown in Fig. 2. The mean speed $\langle v \rangle$ of electrons and the drift velocity W are shown in Fig. 3, where the close values of $\langle v \rangle$ and W within the E/N range between 1 and 10 Td imply the high anisotropy in the velocity distribution. Here, we use the term "anisotropy" to show the deviation of the velocity distribution from the isotropic one due to electric fields. For example, the values of drift velocity W are far smaller than the mean speed $\langle v \rangle$ in conditions of low anisotropy, while the values of $\langle v \rangle$ and W are close between 1 and 10 Td of E/N as are seen in Fig. 3 and imply the high anisotropy. The high anisotropy is usually caused by the excitation collisions, because electrons have to start from a low velocity and will be easily deflected toward the direction of the electric force. The variation of ratios between the two partial energies parallel and perpendicular to the electric field $\langle \varepsilon_{\parallel} \rangle$ and $\langle \varepsilon_{\perp} \rangle$ in Fig. 4 also indicate the variation of anisotropy with E/N . The ratios between the mean free path $\langle G\lambda \rangle$ and the mean forward path $\langle Gx \rangle$ in Fig. 5 also indicate the degree of anisotropy. Numerical data on the electron transport in CF_4 are listed in Table II.

It is observed in Figs. 2~5, that the high mobility does not simply correspond to the high anisotropy. The highest mobility appears at the E/N about 0.2 Td far lower than the range of high anisotropy. On the other hand, the E/N value of the highest flight-time in Fig. 6 is observed at 0.8 Td. FTI analysis can respond to such inquiries through the flight behavior of electrons.

3.1 Flight behavior below 1 Td

In Figs. 8, 9 and 10, normalized starting rate distributions of electrons $\Psi_{Sn}(\varepsilon_0)$ and colliding rates $\Psi_{Cn}(\varepsilon')$, colliding rates for collisions of kind j $\Psi_{Cnj}(\varepsilon')$ and their total $\Psi_{Cn0}(\varepsilon')$ are shown in (a), the colliding rates expressed in Legendre polynomials $\Psi_{Cnl}(\varepsilon')$ in (b), and the velocity distributions in flight $F_l(\varepsilon)$ are shown in (c) for $E/N=0.1, 0.3$ and 0.5 Td, respectively. The first three terms of $\Psi_{Cl}(\varepsilon')$ and $F_l(\varepsilon)$ are shown. At $E/N=0.1$ Td in Fig. 8, most of electrons are confined within a low energy side bank of the momentum transfer cross section, that is the left side of the Ramsauer valley, due to very low value of E/N . Only minority electrons fly over the valley and invade the region above the threshold of vibrational excitation cross section q_{v24} at 0.0539 eV. Accordingly, elastic collision is dominant and the velocity distribution is almost isotropic. This is clearly observed in Fig. 4 in which the two partial mean energies ε_{\parallel} and ε_{\perp} agree to each other at $E/N=0.1$ Td. However, the momentum transfer cross section q_m is decreasing toward the Ramsauer minimum with the increase of energy, and electrons are allowed to fly longer in the forward direction than in the backward. The flight path in this region is obstructed by steeply rising vibrational cross section q_{v13} from about 0.1 to 0.2 eV. Electrons are thus bounded by two walls which lie at 0 and 0.2 eV. In this condition, the lower the energy that electrons start, the larger the possibility of mean forward path $\langle Gx \rangle$. This condition causes electrons to have high mobility in even lower E/N . With the increase of E/N , the increase of mean energy provides lower mean collision frequency and longer mean flight-time for electrons, and the mean flight time takes highest value at about 0.8 Td as is seen in Fig. 6. At the same time, the increase of vibrational excitation rates provides electrons started from low energy range and bring the increase of drift velocity along with increase of anisotropy. Such a situation is clearly observed in Figs 3~10.

As is observed above, a maximum mean flight-time appears at $E/N=0.8$ Td, but a maximum mobility appears at about $E/N=0.2$ Td. It is noticeable that the long flight-

Energy (eV)	q_m Å	Energy (eV)	q_{v24} Å	Energy (eV)	q_{v13} Å	Energy (eV)	q_a Å
9.0	10.8	8.5	0.00745	12.2	0.77		
10.0	11.3	8.6	0.0073	12.4	0.73		
12.0	12.0	8.8	0.00719	12.5	0.71		
15.0	12.4	9.0	0.007	12.6	0.69		
18.0	12.7	10.0	0.0063	12.8	0.66		
20.0	12.5	12.0	0.0053	13.0	0.62		
23.0	12.3	12.2	0.0052	13.2	0.6		
25.0	12.1	12.4	0.00512	13.4	0.58		
28.0	11.6	12.5	0.0051	14.0	0.53		
30.0	11.2	12.6	0.00503	15.0	0.45		
35.0	10.1	12.8	0.00495	17.5	0.35		
40.0	9.1	13.0	0.0049	20.0	0.292		
50.0	7.4	13.2	0.00485	25.0	0.23		
60.0	6.2	13.4	0.00475	30.0	0.19		
70.0	5.45	15.0	0.00425	40.0	0.143		
80.0	4.75	20.0	0.0032	50.0	0.117		
90.0	4.25	25.0	0.0025	60.0	0.1		
100.0	3.85	30.0	0.00212	80.0	0.077		
		40.0	0.0016	100.0	0.063		
		50.0	0.00128				
		60.0	0.00107				

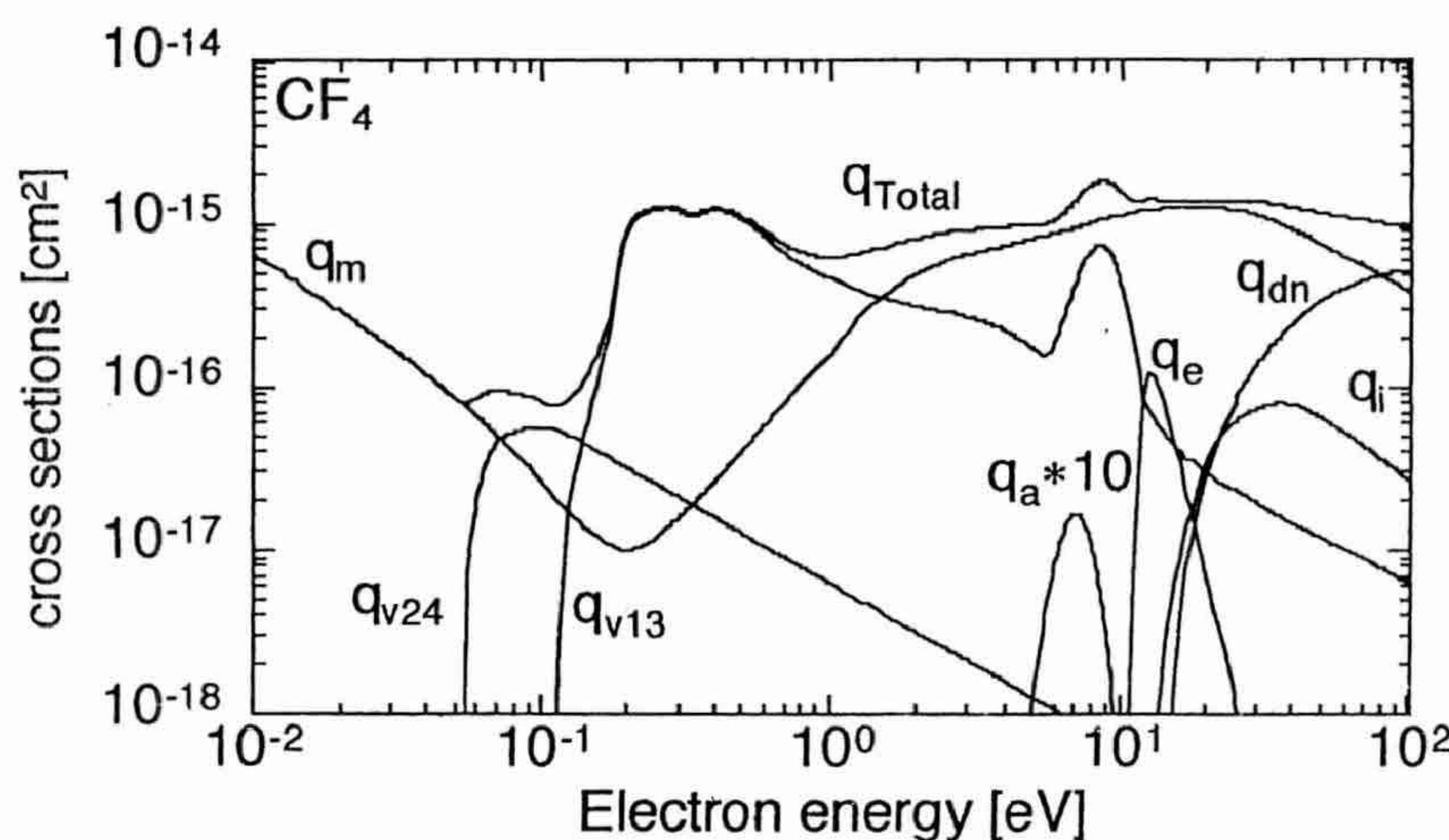


Fig. 1. Revised collision cross sections of CF_4 for electrons reported by M. Hayashi.¹⁰⁾

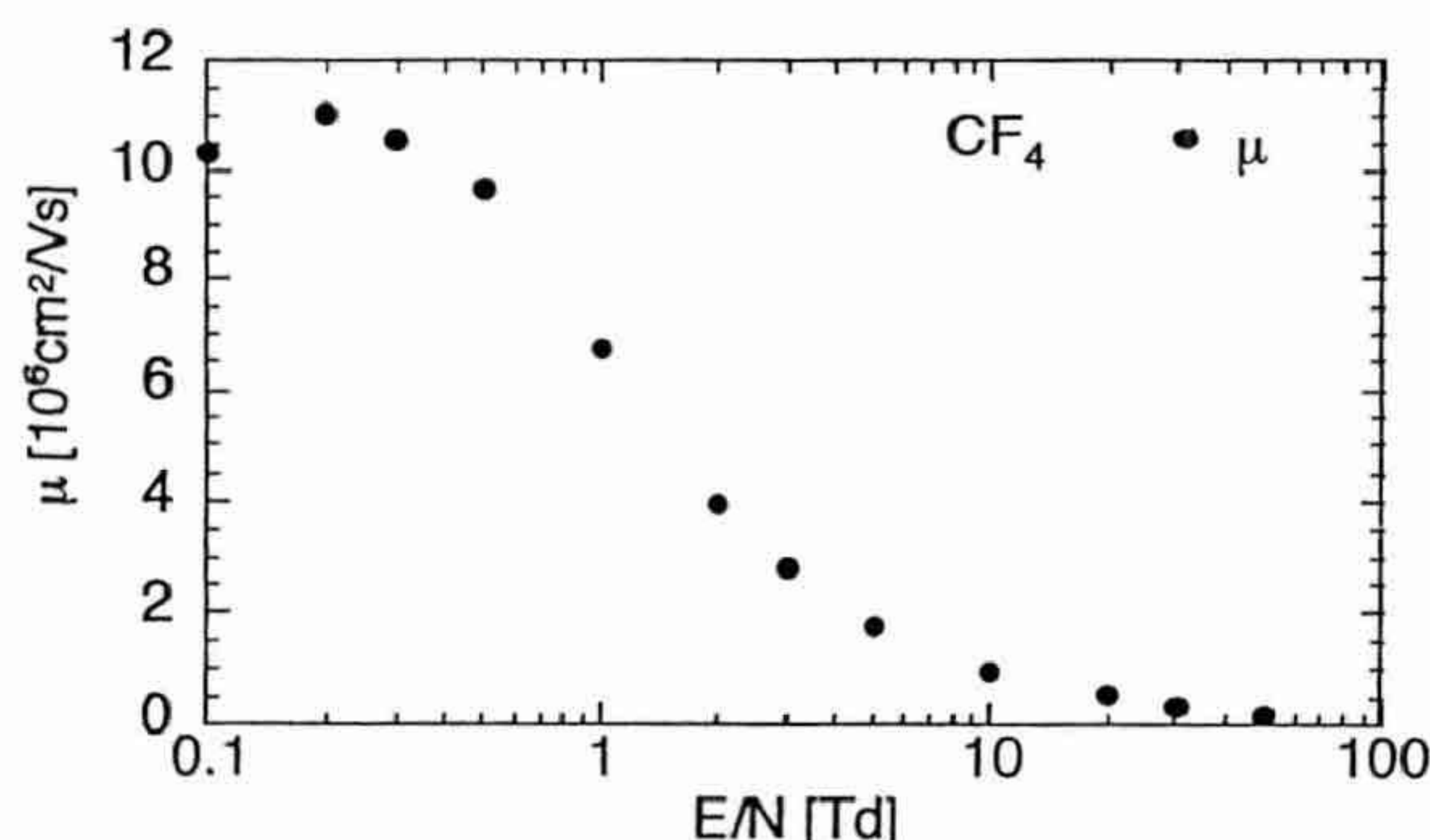


Fig. 2. Electron mobility (μ) curve in CF_4 as a function of reduced field E/N .

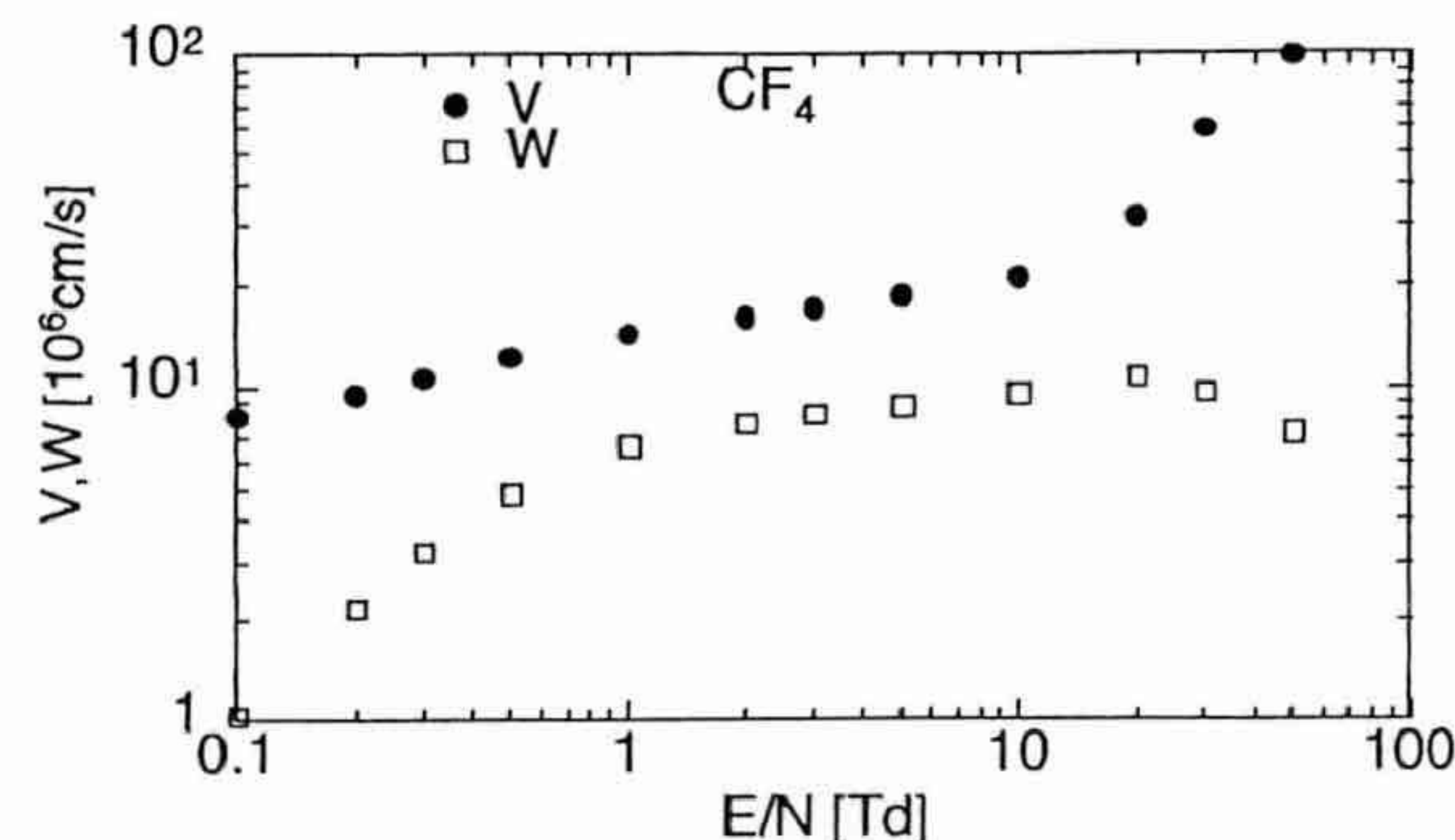


Fig. 3. Mean speed and drift velocity of electrons in CF_4 as functions of reduced field E/N .

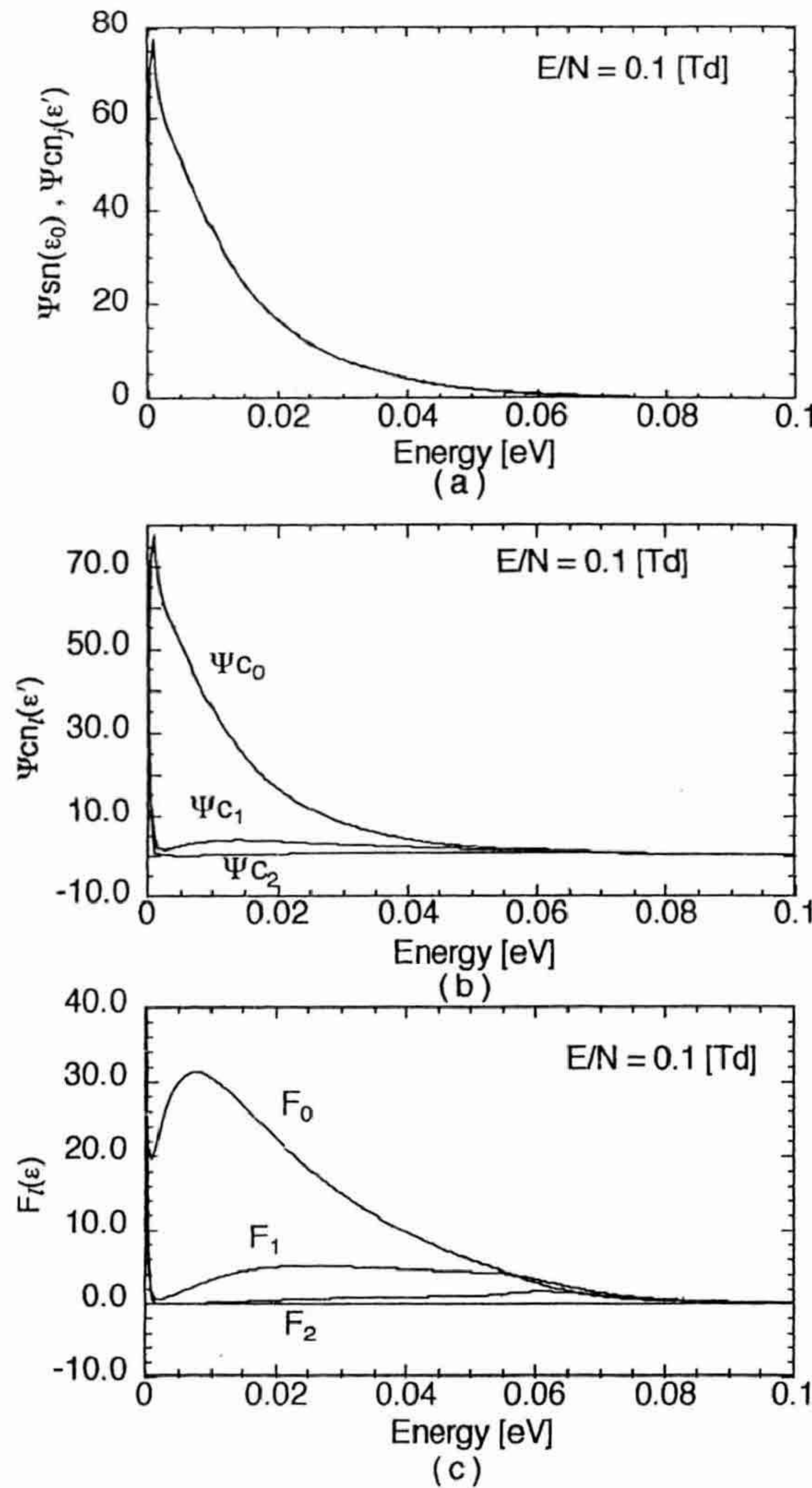


Fig. 8. A set of normalized distributions of starting and colliding rates $\Psi_{Sn}(\varepsilon_0)$ and $\Psi_{Cnj}(\varepsilon')$ in (a), colliding rates $\Psi_{Cnj}(\varepsilon')$ in (b) and of velocity distributions in flight $F_l(\varepsilon)$ in (c) for electrons in CF_4 at $E/N=0.1$ Td.

property of electrons is not so simple but is dependent on the variation of collision frequencies around the starting rate distribution

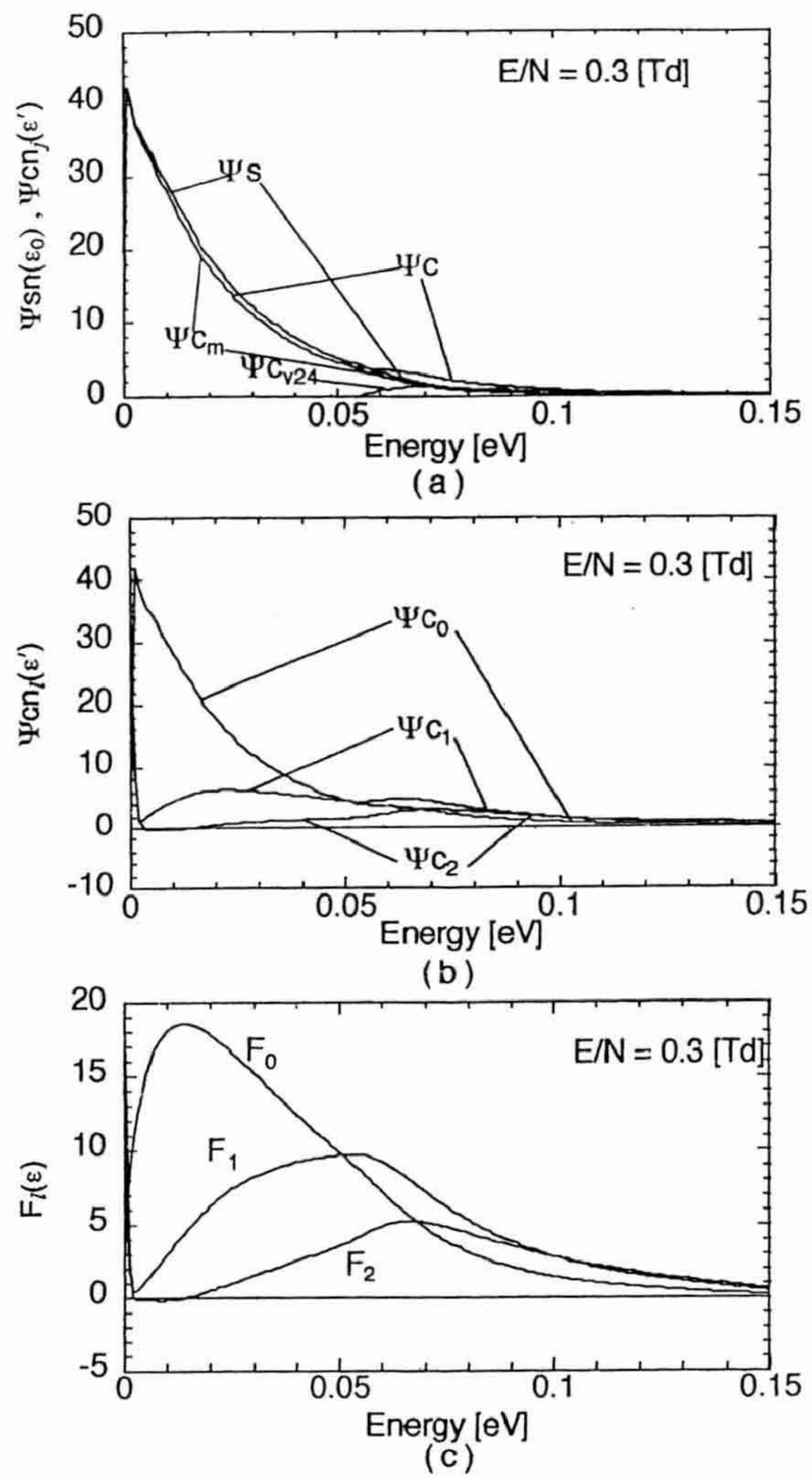


Fig. 9. A set of normalized distributions of starting and colliding rates $\Psi_{Sn}(\varepsilon_0)$ and $\Psi_{Cnj}(\varepsilon')$ in (a), colliding rates $\Psi_{Cnj}(\varepsilon')$ in (b) and of velocity distributions in flight $F_l(\varepsilon)$ in (c) for electrons in CF_4 at $E/N=0.3$ Td.

$\Psi_{Sn}(\varepsilon_0)$. The mean forward path $Gx(\varepsilon_0)$ for an electron isotropically started from ε_0 is given as

$$Gx(\varepsilon_0) = \int_0^\pi \int_0^\infty [v_0 \cos \theta_0 t + (1/2) a t^2] \cdot v_T(\theta_0, t) \cdot \exp \left[- \int_0^t v_T(t'; \varepsilon_0, \theta_0) dt' \right] dt (1/2) \sin \theta_0 d\theta_0, \quad (15)$$

where, the collision frequency of an electron started with ε_0 at θ_0 is written

$$\begin{aligned} v_T(t; \varepsilon_0, \theta_0) &= Nq_T[\varepsilon(t)] v(t) \\ &= Nq_T\{\varepsilon_0 + E[v_0 \cos \theta_0 t + (1/2) a t^2]\} [v_0^2 + v_0 \cos \theta_0 a t + a^2 t^2]^{1/2}. \end{aligned} \quad (16)$$

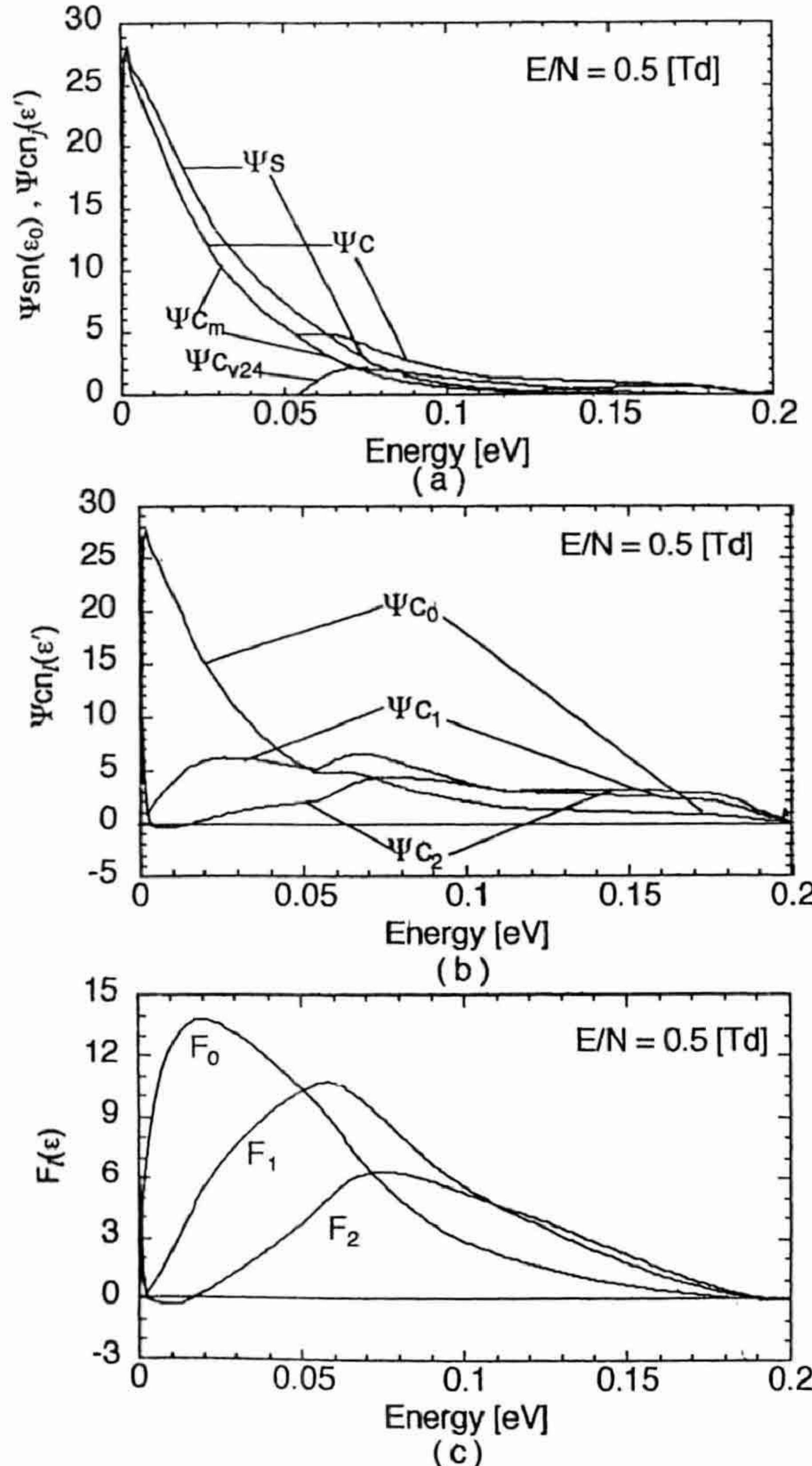


Fig. 10. A set of normalized distributions of starting and colliding rates $\Psi_{Sn}(\varepsilon_0)$ and $\Psi_{Cn_j}(\varepsilon')$ in (a), colliding rates $\Psi_{Cn_l}(\varepsilon')$ in (b) and of velocity distributions in flight $F_l(\varepsilon)$ in (c) for electrons in CF_4 at $E/N=0.5$ Td.

The collision frequency $\nu_T(t'; \varepsilon_0, \theta_0)$ is not constant but time dependent, and the mean free path is dependent on ε_0 and θ_0 corresponding to the condition $d\nu_T(\varepsilon)/d\varepsilon$ being positive or negative. For electrons in CF_4 in low E/N , $d\nu_T(\varepsilon)/d\varepsilon < 0$, and electrons fly long in forward direction than backwards. The discrepancy of the E/N values giving the minimum mean collision frequency at about 0.8 Td and the maximum mobility at 0.2 Td is caused by the flight behavior of electrons in this low energy region.

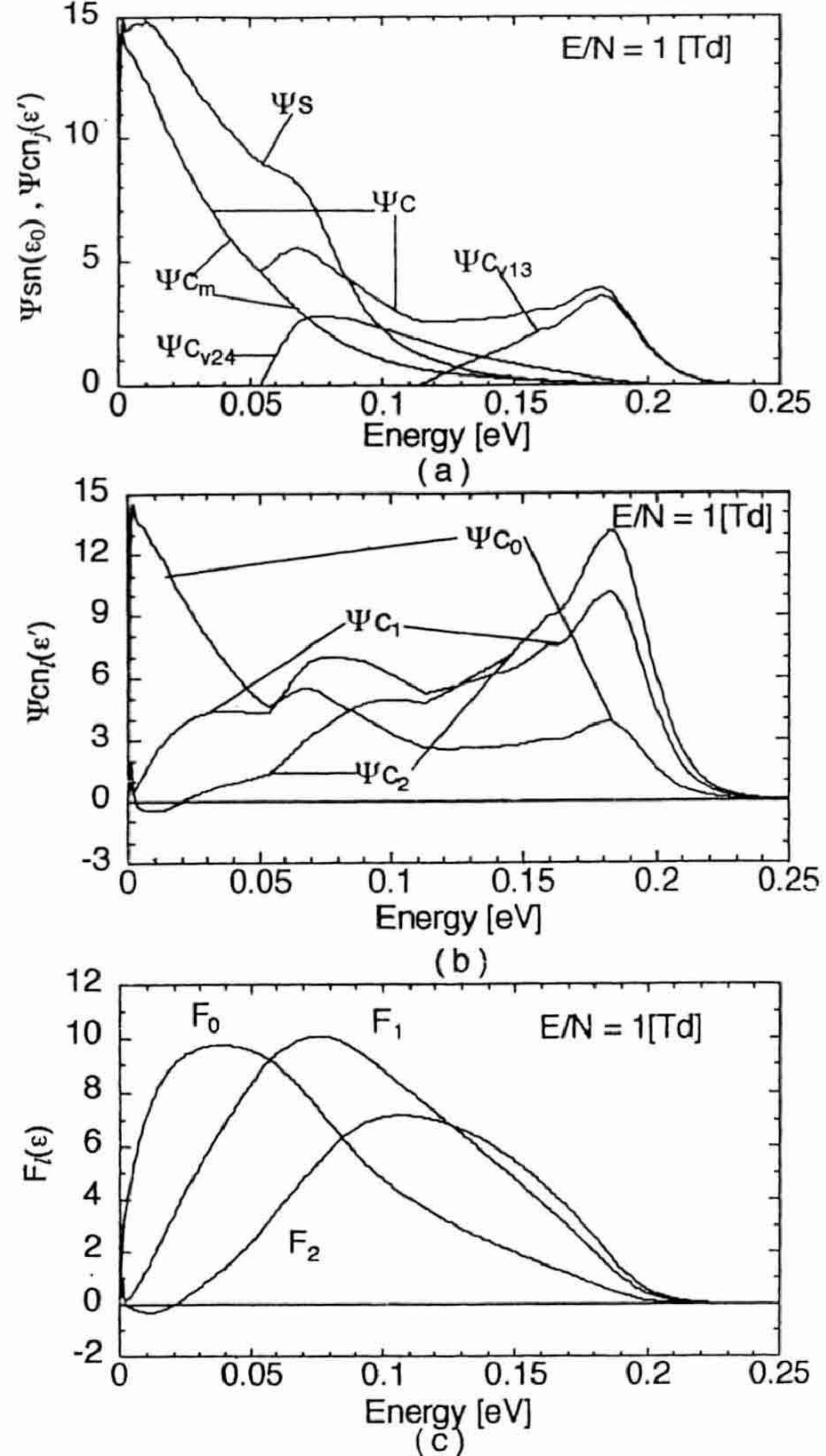


Fig. 11. A set of normalized distributions of starting and colliding rates $\Psi_{Sn}(\varepsilon_0)$ and $\Psi_{Cn_j}(\varepsilon')$ in (a), colliding rates $\Psi_{Cn_l}(\varepsilon')$ in (b) and of velocity distributions in flight $F_l(\varepsilon)$ in (c) for electrons in CF_4 at $E/N=1$ Td. Between $\Psi_{Sn}(\varepsilon_0)$ and $\Psi_{Cn_j}(\varepsilon')$, energy loss due to vibrational excitations are observed.

3.2 Flight behavior between 1 and 10 Td

Four sets of normalized distributions $\Psi_{Sn}(\varepsilon_0)$ and $\Psi_{Cn_j}(\varepsilon')$ in (a), $\Psi_{Cn_l}(\varepsilon')$ in (b) and $F_l(\varepsilon)$ in (c) for $E/N=1, 3, 5$ and 10 Td are shown in Figs. 11 ~ 14, respectively. Main part of $\Psi_{Cn0}(\varepsilon')$ enters into the region of high cross section for vibrational excitation q_{v13} with the increase of E/N . Electrons those made vibrational excitation shown by $\Psi_{Cv13}(\varepsilon')$ around 0.2 eV in (a) lose the threshold energy 0.113 eV and form $\Psi_{Sn}(\varepsilon_0)$ which has a peak at about 0.1 eV. Most of electrons started with

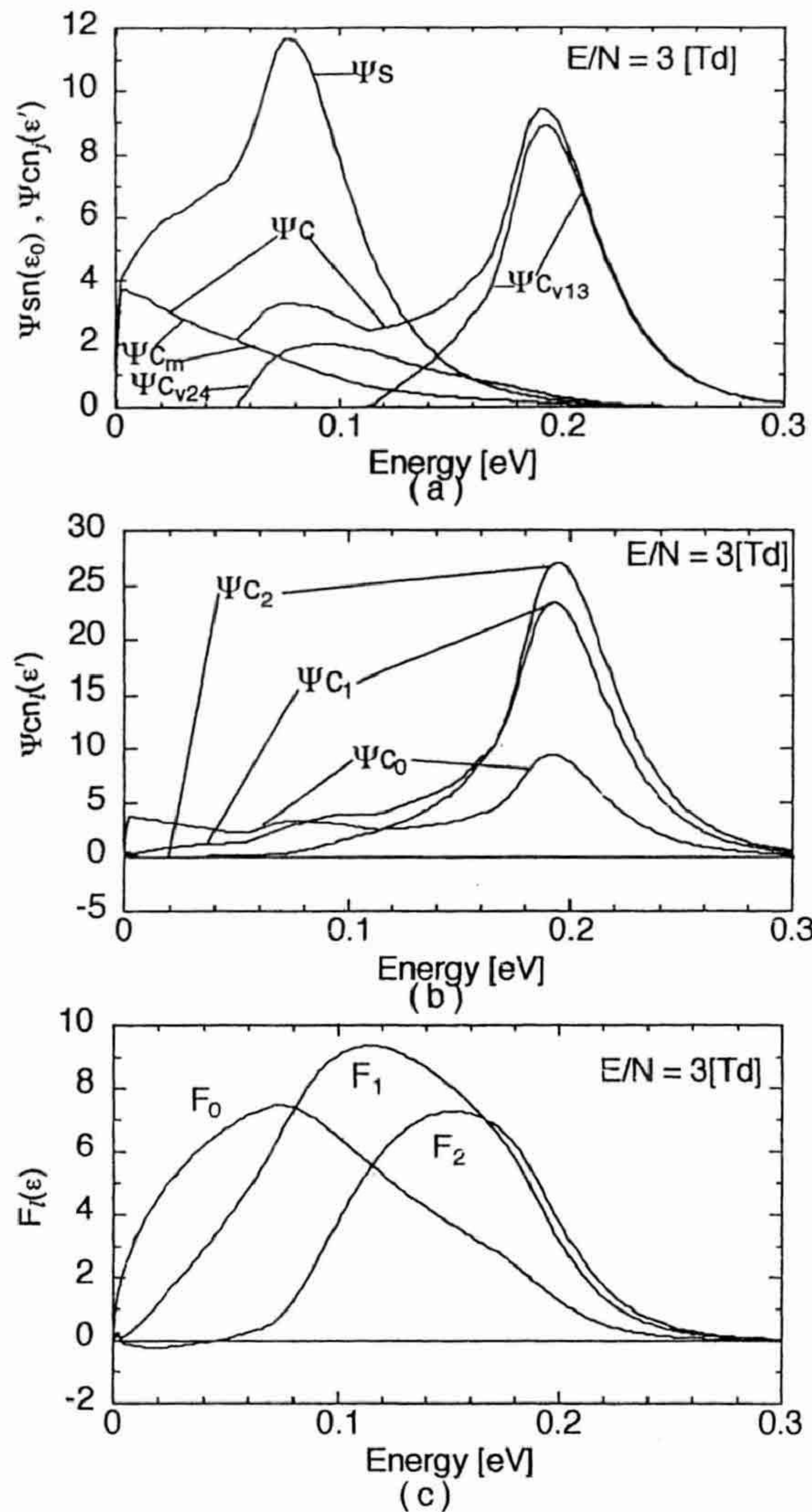


Fig. 12. A set of normalized distributions of starting and colliding rates $\Psi_{Sn}(\varepsilon_0)$ and $\Psi_{CnJ}(\varepsilon')$ in (a), colliding rates $\Psi_{CnJ}(\varepsilon')$ in (b) and of velocity distributions in flight $F_l(\varepsilon)$ in (c) for electrons in CF_4 at $E/N=3$ Td.

this $\Psi_{Sn}(\varepsilon_0)$ fly long over the Ramsauer valley in forward direction forming strongly anisotropic energy distributions $F_l(\varepsilon)$. As are observed in Figs. 11~14, the distributions $F_1(\varepsilon)$ generally surpass $F_0(\varepsilon)$, and distributions $F_2(\varepsilon)$ also have large values. In lower energy range below 0.1 eV, $F_2(\varepsilon)$ in Figs. 13 and 14 have negative values. This is due to that $\Psi_S(\varepsilon_0)$ has its peak at about 0.1 eV, the backward starting components turn to transverse direction below 0.1 eV and give negative values in $F_2(\varepsilon)$. On the other hand, electrons started in higher energy tail of $\Psi_S(\varepsilon_0)$ can not

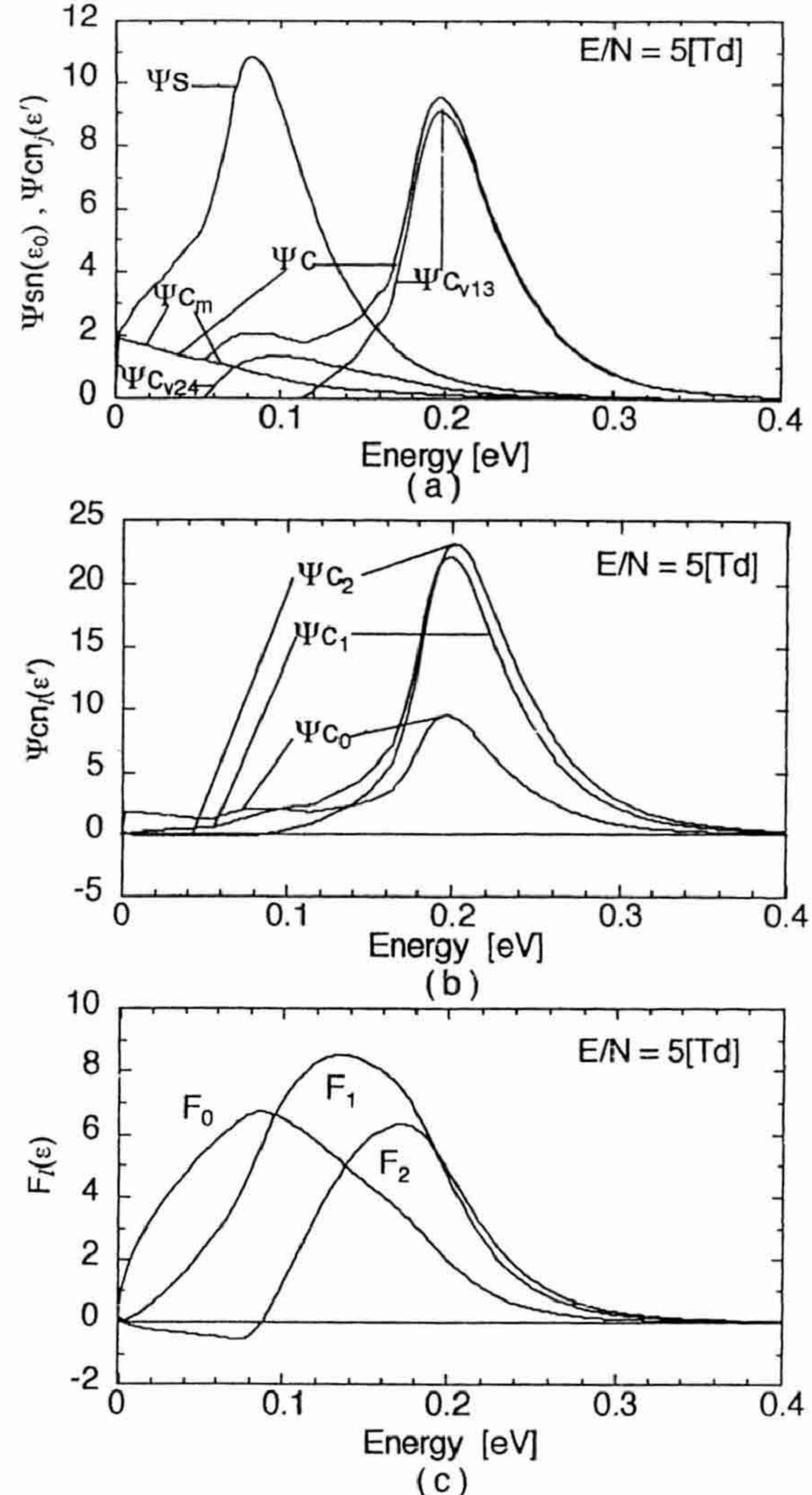


Fig. 13. A set of normalized distributions of starting and colliding rates $\Psi_{Sn}(\varepsilon_0)$ and $\Psi_{CnJ}(\varepsilon')$ in (a), colliding rates $\Psi_{CnJ}(\varepsilon')$ in (b) and of velocity distributions in flight $F_l(\varepsilon)$ in (c) for electrons in CF_4 at $E/N=5$ Td.

fly long. The detail of flight behavior for an electron isotropically started from ε_0 is observed in the velocity dispersion functions $H_0(\varepsilon', \varepsilon_0)$ at 3 Td in Fig. 15 shown as an example. The flight behavior is also observed in the mean forward path $Gx(\varepsilon_0)$ in Fig. 16 for an electron isotropically started from ε_0 . In both figures, the difference in the flight behavior below and above the turning point 0.2 eV is evident.

Throughout the E/N range from 1 to 10 Td, strongly anisotropic velocity distributions are clearly observed in the small ratios be-

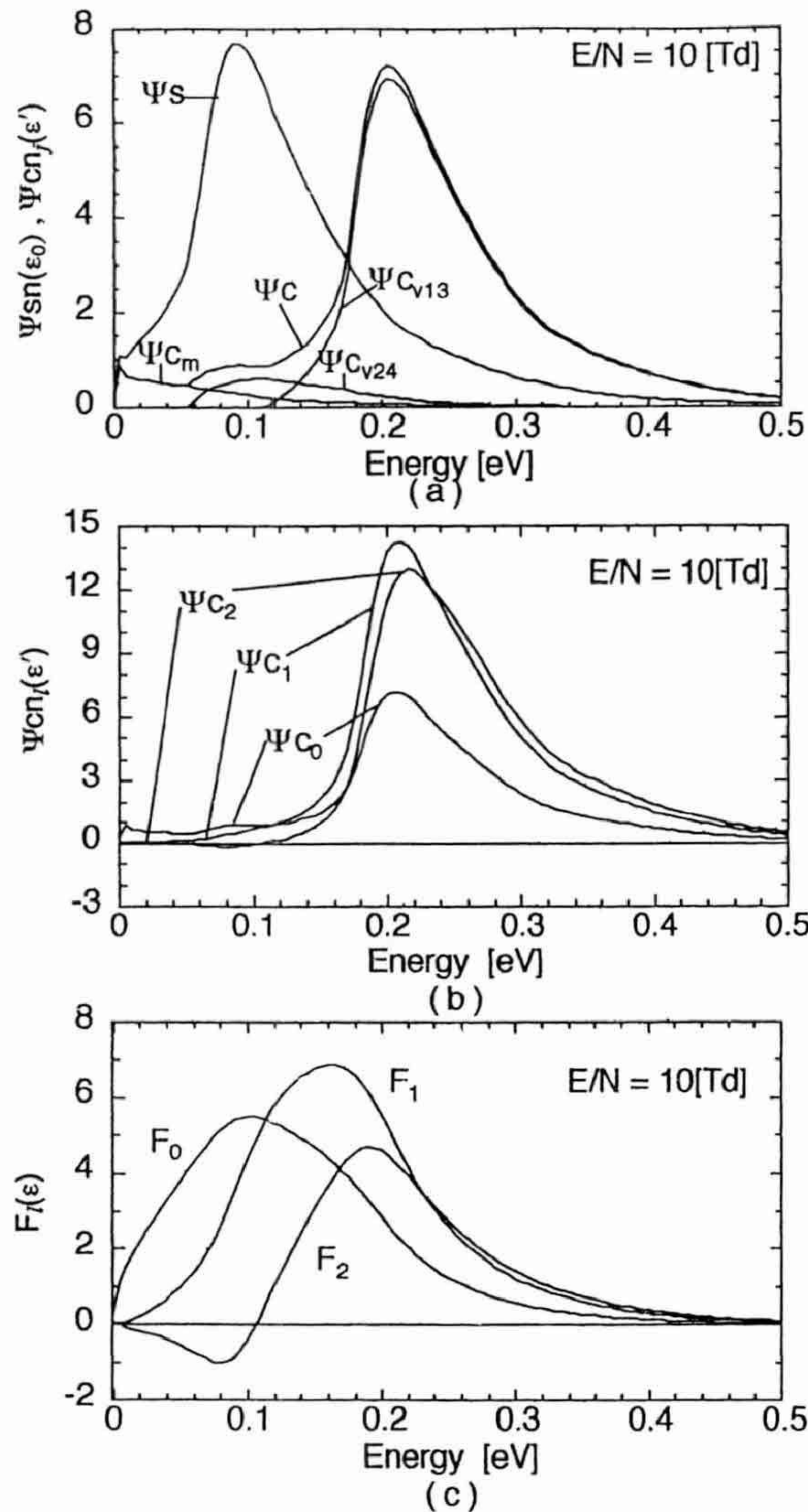


Fig. 14. A set of normalized distributions of starting and colliding rates $\Psi_{Sn}(\varepsilon_0)$ and $\Psi_{Cn,j}(\varepsilon')$ in (a), colliding rates $\Psi_{Cn,l}(\varepsilon')$ in (b) and of velocity distributions in flight $F_l(\varepsilon)$ in (c) for electrons in CF_4 at $E/N=10$ Td.

tween $\langle v \rangle$ and W in Fig. 3, between $\langle G\lambda \rangle$ and $\langle Gx \rangle$ in Fig. 5 and the large ratio between ε_{\parallel} and ε_{\perp} in Fig. 4. The ratios $\langle v \rangle/W$, $\varepsilon_{\parallel}/\varepsilon_{\perp}$ and $\langle G\lambda \rangle/\langle Gx \rangle$ are maintained almost constant through 1 and 10 Td although the values of $\langle G\lambda \rangle$ and $\langle Gx \rangle$ are already decreasing due to the decrease of flight of electrons from the low energy region. While, the drift velocity W continues to increase with slightly positive gradient to E/N due to the increase of E/N .

When most of electrons tend to collide at higher energy range with the increase of E/N , that is, the relative number of electrons start-

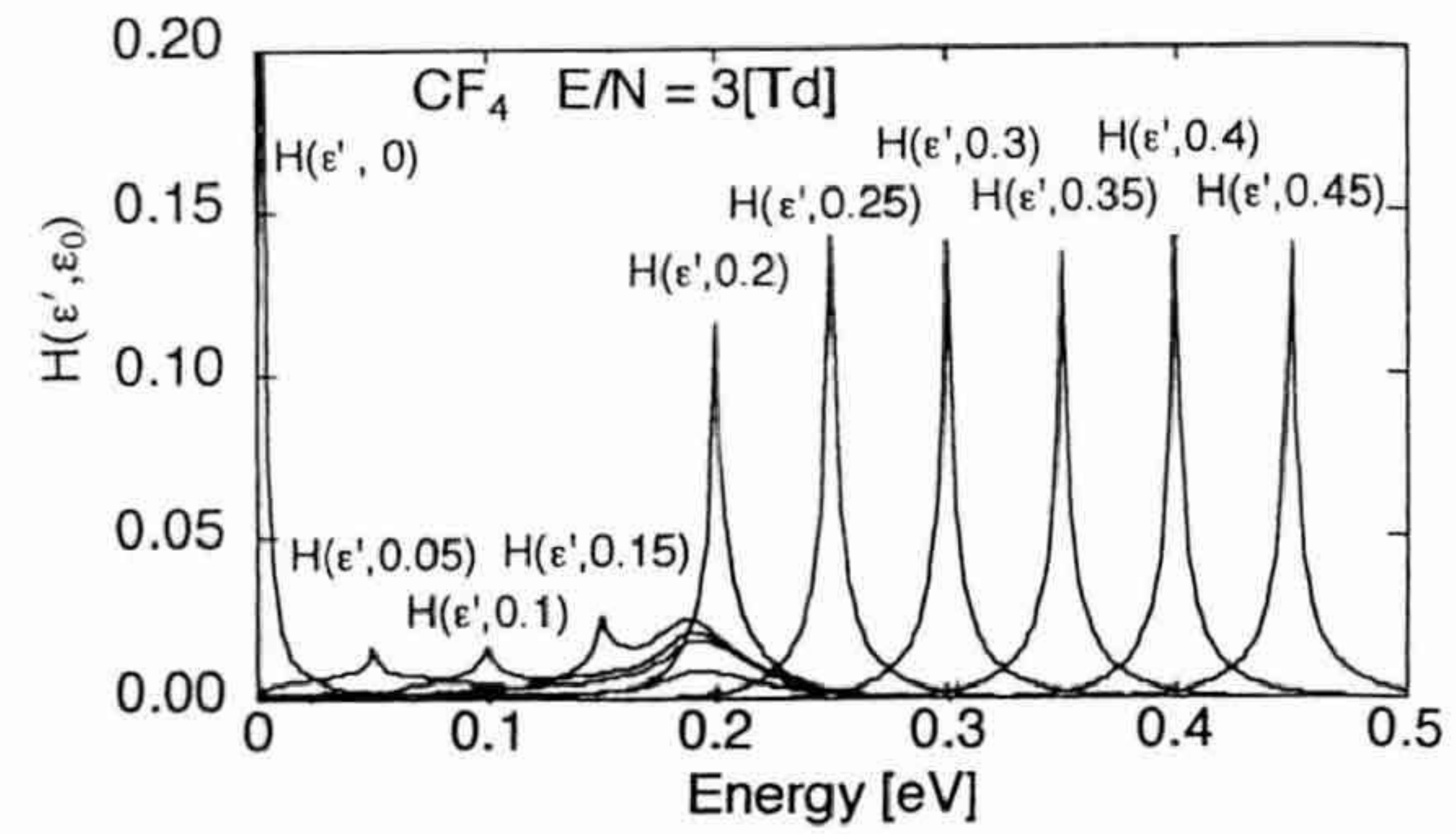


Fig. 15. Energy dispersion function in flight $H(\varepsilon', \varepsilon_0)$ which gives the probability of velocity dispersion in a flight for an electron started from ε_0 at $E/N=3$ Td.

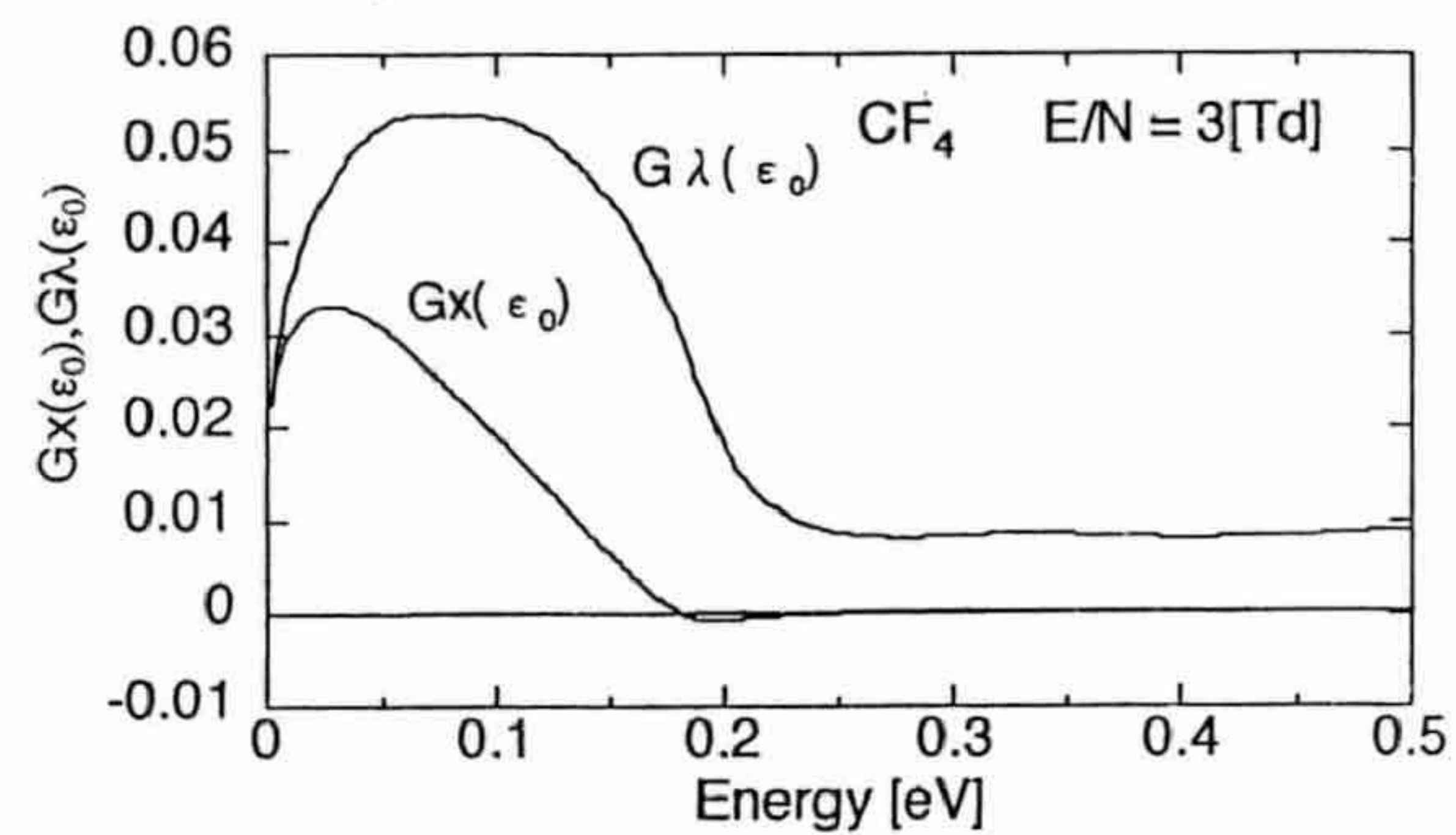


Fig. 16. Electron transport functions $G\lambda(\varepsilon_0)$ and $Gx(\varepsilon_0)$, the mean free path and the mean forward displacement in a flight for an electron started from ε_0 at $E/N=3$ Td.

ing from the low energy region decreases rapidly and the mean axial path $\langle Gx \rangle$ in Fig. 16 decreases. Then the maximum in the drift velocity appears at about $E/N=20$ Td.

3.3 Flight behavior above 20 Td

With the increase of E/N above 20 Td, majority of electrons tends to collide at higher energies of vibrational excitation cross section q_{v13} , and the high energy tail of normalized starting rate distribution $\Psi_{Sn}(\varepsilon_0)$ extends over several eV until the flight of electrons are obstructed by the next sharp rise of q_{v13} at about 8 eV. Possible flight paths from the higher energy are shorten due to the second increase of q_{v13} . Therefore, the drift velocity decreases with the increase of E/N . The decreasing region of drift velocity is called the region of negative differential conductivity.¹⁾ The distributions $\Psi_{Sn}(\varepsilon_0)$ and $\Psi_{Cn,j}(\varepsilon')$ in (a), $\Psi_{Cl}(\varepsilon')$ in (b) and $F_l(\varepsilon)$ in (c) for $E/N=30$ and 50 Td are

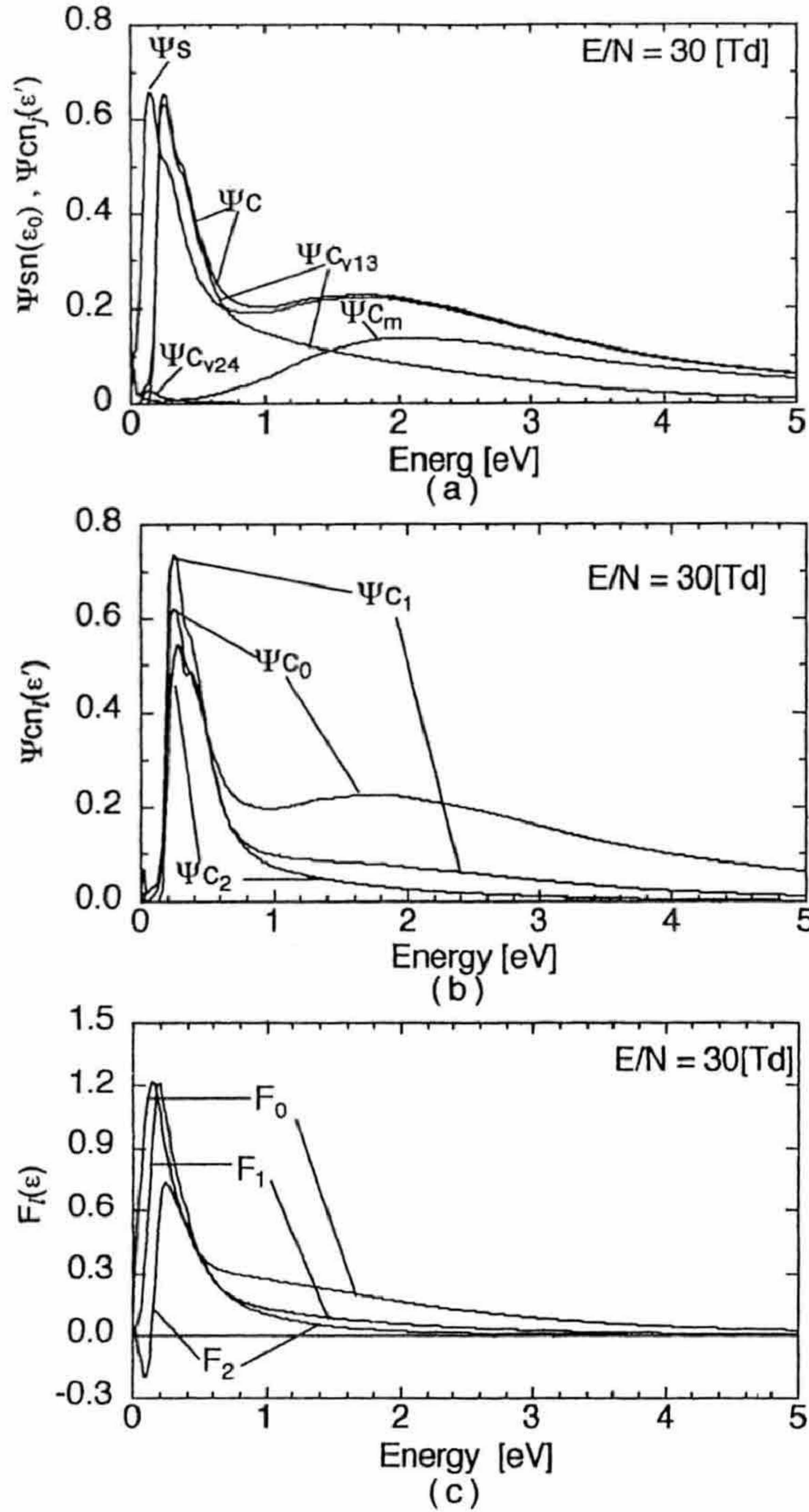


Fig. 17. A set of normalized distributions of starting and colliding rates $\Psi_{Sn}(\varepsilon_0)$ and $\Psi_{Cn,j}(\varepsilon')$ in (a), colliding rates $\Psi_{Cn,l}(\varepsilon')$ in (b) and of velocity distributions in flight $F_l(\varepsilon)$ in (c) for electrons in CF_4 at $E/N=30$ Td.

shown in Figs. 17 and 18, respectively. In Fig. 19, the mean free path and mean forward path for an electron started from ε_0 , $G\lambda(\varepsilon_0)$ and $Gx(\varepsilon_0)$ at $E/N=30$ Td are shown, where the depression of the forward path $Gx(\varepsilon_0)$ above 0.2 eV are clearly observed. Note that the energy gain in a flight $EGx(\varepsilon_0)$ which appears in Fig. 19 gives the mean value of $\int (\varepsilon' - \varepsilon_0) H_0(\varepsilon', \varepsilon_0) d\varepsilon'$ observed in the energy dispersion functions $H_0(\varepsilon', \varepsilon_0)$ in Fig. 20 at $E/N = 30$ Td, for example.

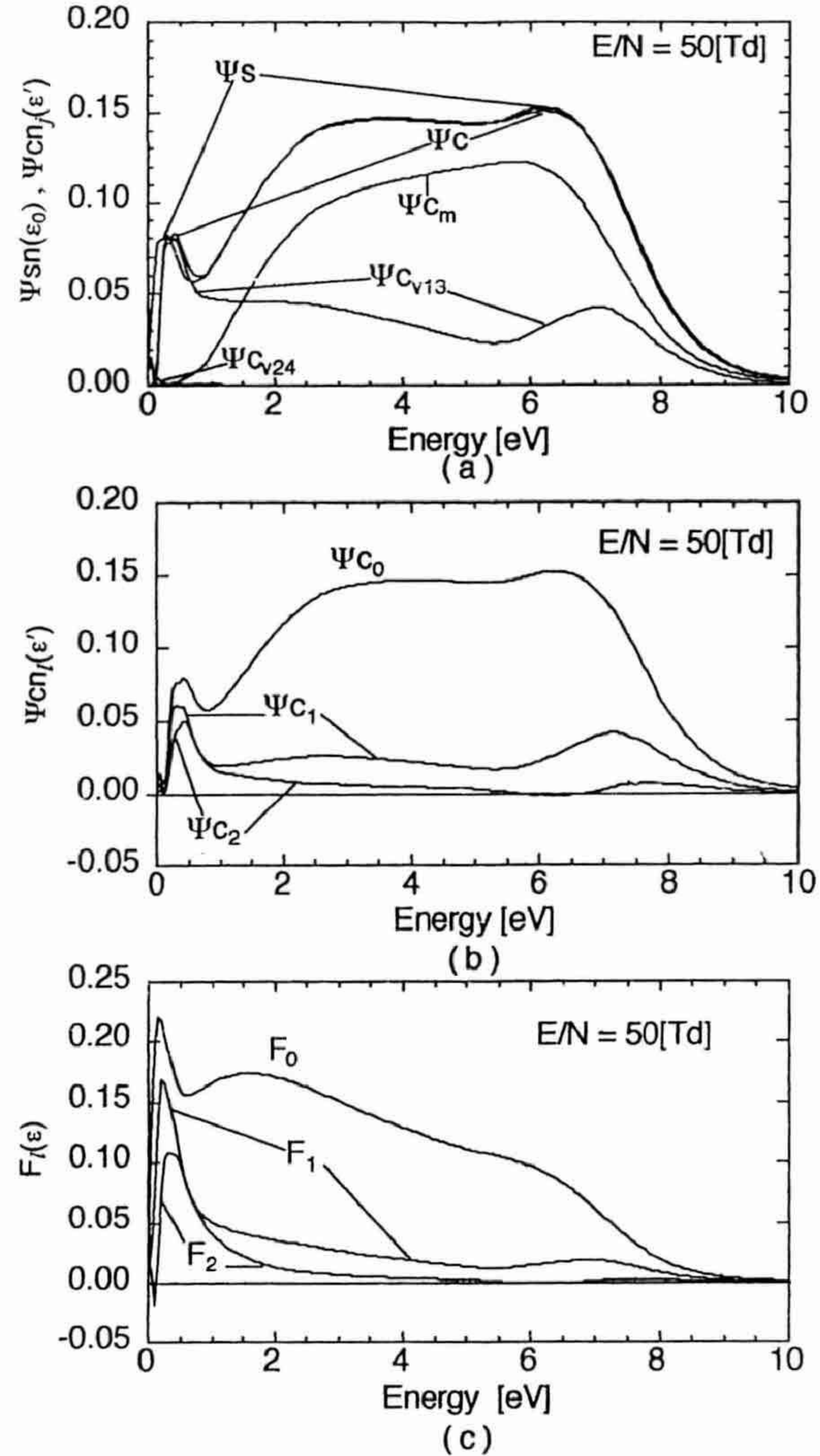


Fig. 18. A set of normalized distributions of starting and colliding rates $\Psi_{Sn}(\varepsilon_0)$ and $\Psi_{Cn,j}(\varepsilon')$ in (a), colliding rates $\Psi_{Cn,l}(\varepsilon')$ in (b) and of velocity distributions in flight $F_l(\varepsilon)$ in (c) for electrons in CF_4 at $E/N=50$ Td.

3.4 Comparison with previous study

Research for the transport properties of ions and electrons have been considered directly from the collision cross section or the collision frequency. If the same is done here, the discrepancy between the mobility and the flight-time might have not been understood so clearly. FTI analyses have shown the electron flight behavior in detail.

Petrovic *et al.* and Robson discussed the NDC to be due to the existence of excitation collision even without the Ramsauer Townsend minimum in the momentum transfer cross section. Although their model was of

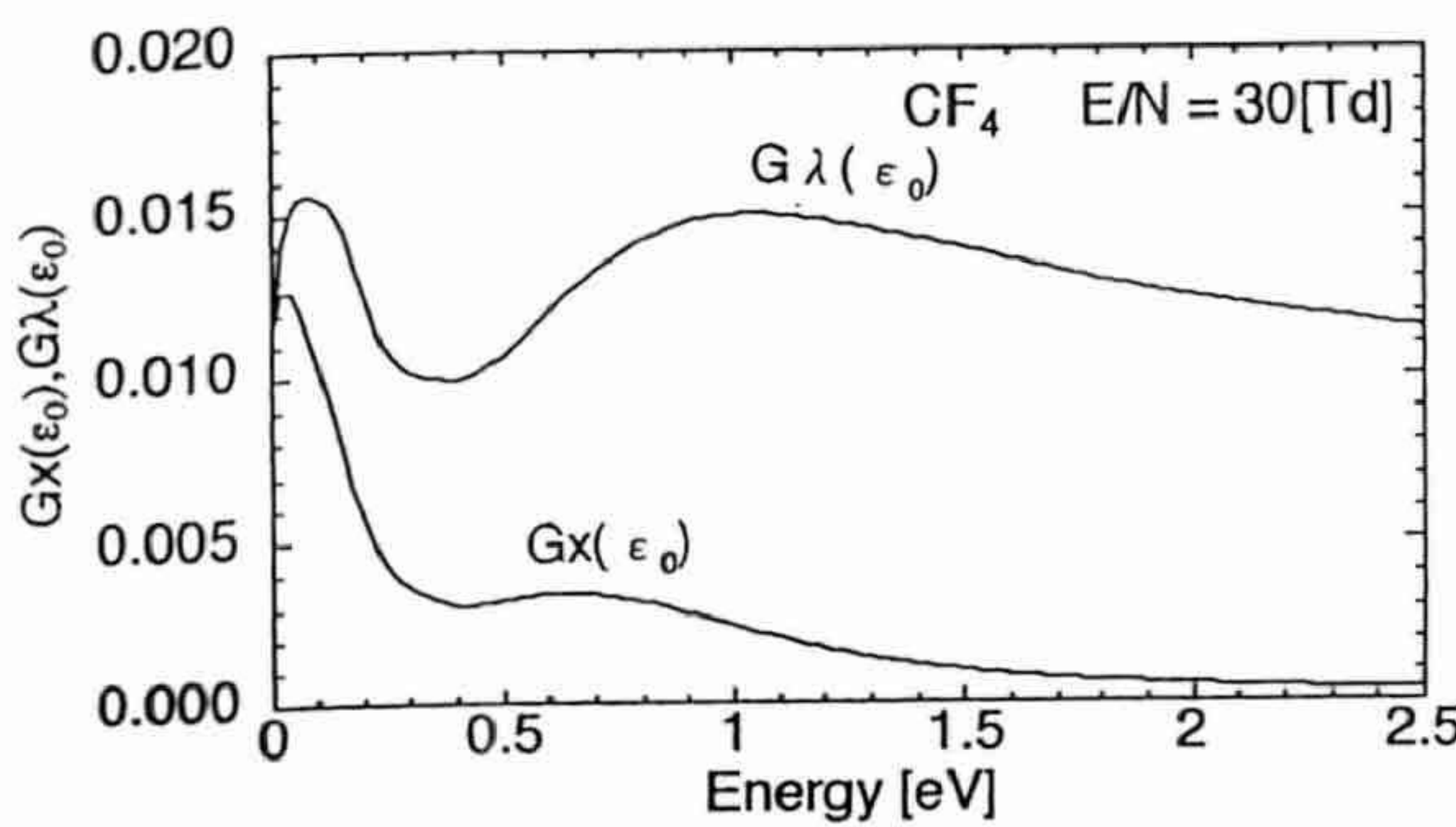


Fig. 19. Electron transport functions $G\lambda(\varepsilon_0)$ and $Gx(\varepsilon_0)$, the mean free path and the mean forward displacement in a flight for an electron started from ε_0 at $E/N=30$ Td.

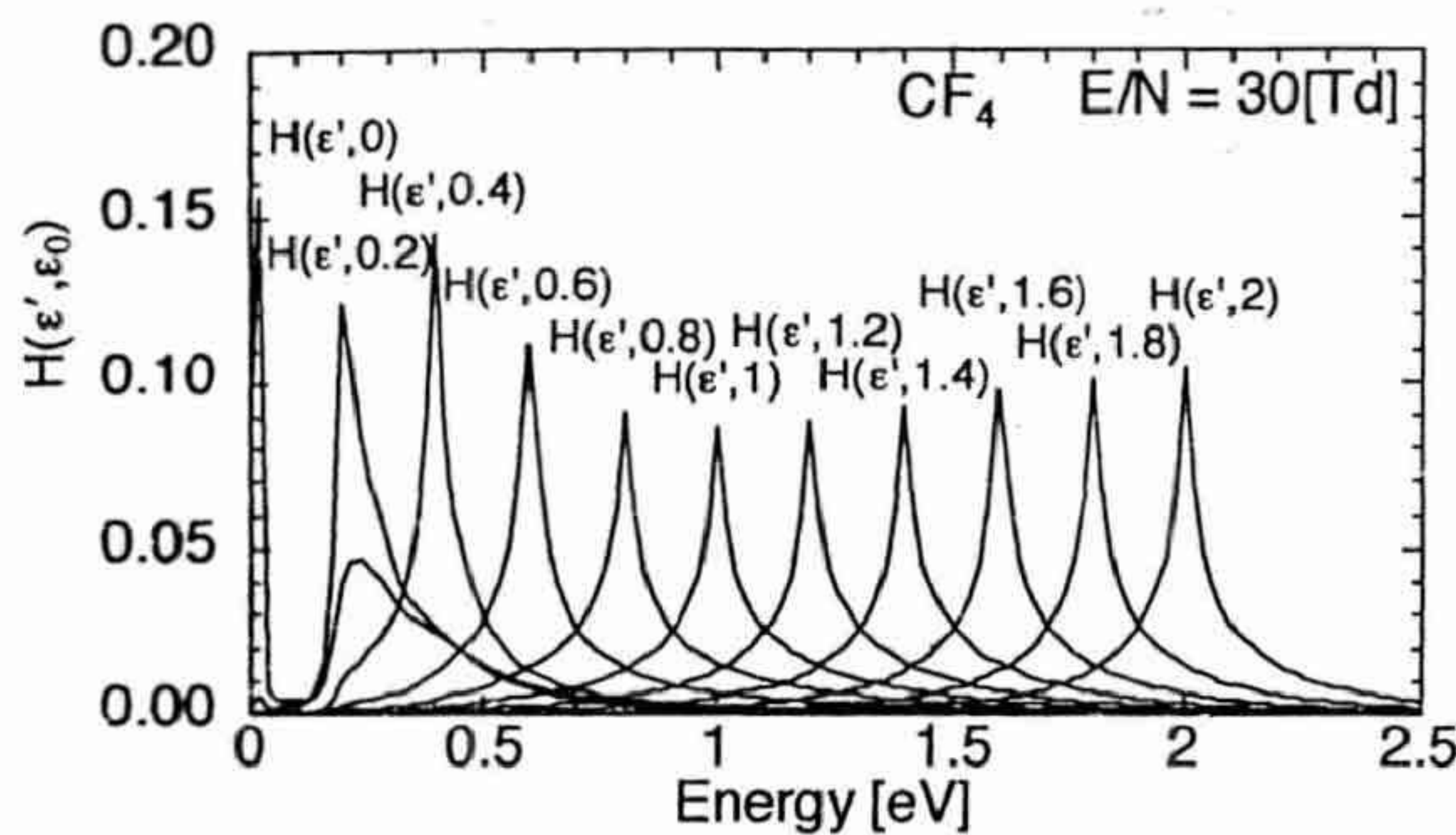


Fig. 20. Energy dispersion function in flight $H(\varepsilon', \varepsilon_0)$ which gives the probability of velocity dispersion in a flight for an electron started from ε_0 at $E/N=30$ Td.

low excitation cross section, but clearly explained the NDC at an E/N region. Such NDC is considered to be brought by the drift velocity enhancement in the lower E/N due to the existence of excitation cross section at a limited energy range, and NDC appears in the recovery path to the intrinsic curve of W with E/N, for example, proportional to $(E/N)^{1/2}$ for the constant elastic cross section model. In CF₄, however, the effect of vibrational excitation is far larger than that in Petrovic and Robson's model at the point acting as the barrier with steeply rising to high value. The appearance property of NDC is dependent on the shape of excitation cross section as they explained.

§4. Conclusion

Adopting Hayashi's revised cross sections, electron transport properties in CF₄ have been analysed over a wide range of reduced electric field E/N from 0.1 to 50 Td with the FTI

method proposed by the authors. The FTI method is capable to analyse the transport properties of electrons in steady state by considering the full flight behavior with sufficient accuracy and stability for arbitrary cross sections and E/N values.

It has been made clear that the mobility of electrons is dependent not only on the value of $v(\varepsilon)$ but also on the gradient $dv(\varepsilon)/d\varepsilon$. The peak energy of $\Psi_{Sn}(\varepsilon_0)$ also gives large influence to the mean axial path up to the barrier of q_{v24} and q_{v13} . The lower peak energy of $\Psi_{Sn}(\varepsilon_0)$ will give higher mobility. The difference in the E/N values giving maxima in mobility and mean flight-time is caused by these circumstances. Particularly, the discrepancy becomes large when the $\Psi_{Sn}(\varepsilon_0)$ is concentrated within a narrow energy range.

The drift velocity of electrons increases with E/N through the increase of relative number of excitation collision compared to elastic collision as far as the inelastic loss energy is comparatively large. The excitation collision make electrons start from the low energy region and make fly long in forward direction. Accordingly, the excitation cross section acts as the enhancer of drift velocity at the E/N region.

When many electrons tend to overcome the barrier and collide in higher energy range with the increase of E/N, the starting rate $\Psi_{Sn}(v_0)$ shifts to higher energy. Accordingly, the mean axial flight path $\langle Gx \rangle$ decreases, and the drift velocity curve begins to descend giving a region of negative differential conductivity NDC. It is considered that the NDC is caused mainly as the result of irregular enhancement of drift velocity W at an E/N region lower than that of NDC, although the shape of W-E/N curve will depend on the conditions in the neighbor of the NDC.

The present analysis is based on the assumption of isotropic scattering of electrons in the laboratory frame, which make the FTI analyses easy allowing the isotropic starting rate $\Psi_{Sn}(v_0)$. If an anisotropic scattering has to be considered, the verification for the usual procedure of analysis using the momentum transfer cross section will be necessary first.

References

- 1) Z. Lj. Petrovic, R. W. Crompton and G. N.

- Haddad: Aust. J. Phys. **37** (1984) 23.
- 2) R. E. Robson: Aust. J. Phys. **37** (1984) 35.
- 3) M. S. Naidu and A. N. Prasado: J. Phys. D: Appl. Phys. **5** (1972) 983.
- 4) L. G. Christophorou, D. L. McCorkle, D. L. Maxey and L. G. Carter: Nucl. Inst. Methods **163** (1979) 141.
- 5) M. Kurachi and Y. Nakamura: *Proc. 13th Symp. on ISIAT '90, Tokyo* (1990) 205.
- 6) Y. Nakamura: Papers of Technical Meeting on Electrical Discharges, (ED-92-145) (1992), IEE Japan [in Japanese].
- 7) M. Hayashi: *Swarm Studies and Inelastic Electron-Molecule Collisions*, ed. L. C. Pitchford, B. V. Mackoy, A. Chutian and S. Trajmer (Springer-Verlag, 1987) p. 187.
- 8) Nakamura: Papers of Technical Meeting of Electrical Discharges, ED-88-58, IEE of Japan [in Japanese].
- 9) Nakamura: Papers of Technical Meeting of Electrical Discharges, ED-89-71, IEE of Japan [in Japanese].
- 10) M. Hayashi: *Handbook of Plasma Material Science*, Ohm, p. 762.
- 11) N. Ikuta and Y. Murakami: J. Phys. Soc. Jpn. **56** (1987) 115.
- 12) M. Fukutoku and N. Ikuta: J. Phys. Soc. Jpn. **59** (1990) 2727.
- 13) N. Ikuta and S. Nakajima: Trans. IEE of Japan, **113-A** (1993) 83.